Volume 10, Issue 1, 2020, 4837 - 4845 ISSN 2069-5837
Biointerface Research in Applied Chemistry
www.BiointerfaceResearch.com
https://doi.org/10.33263/BRIAC101.837845
Original Research Article Open Access Journal
Received: 16.10.2019 / Revised: 15.12.2019 / Accepted: 18.12.2019 / Published on-line: 28.12.2019

Effect of nano metal oxides on heme molecule: molecular and biomolecular approaches

Ahmed M. Bayoumy [1], Hanan Elhaes [2], Osama Osman [3], Kholmirzo T. Kholmurodov [4], Tarek Hussein [5], Medhat A. Ibrahim [3]

[1]Physics Department, Biophysics Branch, Faculty of Science, Ain Shams University, 11566, Cairo, Egypt
[2]Physics Department, Faculty of Women for Arts, Science and Education, Ain Shams University, 11757 Cairo, Egypt
[3]Spectroscopy Department, National Research Centre, 33 El-Bohouth Str. 12622 Dokki, Giza, Egypt
[4]Dubna State University, 141982, Universitetskaya 19, Dubna, Russia.
[5]Physics Department, faculty of Science, Cairo University, 12613 Giza Egypt.

*corresponding author e-mail address: ***medahmed6@yahoo.com*** | Scopus ID 8641587100

ABSTRACT

Interaction of components of living cells with various nanomaterials in the gas phase has been one of extensive concern since they become intensively utilized in various life aspects. This work is carried out to investigate the interaction between heme molecule, as the main component of hemoglobin, with several familiar and non-familiar divalent structures such as O_2, CO_2, CO, MgO, CoO, NiO, CuO and ZnO. Geometry optimization processes as well as QSAR descriptors are conducted using semiemprical quantum mechanical calculations at PM6 level. Results illustrate that adsorbing O_2 and CO on heme lowers their TDM helping heme in performing its transportation function and not interacting with other species. On the other hand, when CoO and ZnO interacting with heme the TDM of the resultant structures increase greatly reflecting high reactivity which may interact with other species more than performing its function. Therefore, interacting species other than O_2 may disturb the transportation function of heme structure. QSAR data of IP regarding interaction of O_2 with heme ensure the TDM result that reflects lowering its activity. IP of H-CO adsorbed is the lowest indicating high reactivity while those of H-O_2, H-CO_2, H-MgO and H-NiO in the complex form are the highest values indicating that it is difficult to form a complex structure with them. Therefore, heme interactions with structures rather than O_2 and CO_2 affects negatively its function as gas transporter.

Keywords: *Heme, PM6, Molecular modeling, Nano metal oxides, QSAR.*

1. INTRODUCTION

Nanotechnology facilitates and even controls the process of assembling materials at nanoscale materials. It is well recognized that materials in nanoscale emerge among the focal points of modem research [1-3]. Developments in nanomaterials are not limited to techniques for preparations and investigations; different applications, but also include the theories dealing with interactions in nanoscale [4-5]. As compared with bulk materials, the nanoscale materials have increased surface to volume ratio, this in turn increases the mechanical strength beside their physicochemical properties [6]. With the help of nanoscale engineering, it is possible to design biomaterials with certain dimensions and organization, which enabling new directions for manipulating cellular behavior [7-8]. In spite of this applications there are some reports against nanotechnology, there is a report about the genotoxicity of fullerene. Some others are reporting the possible toxicity of nanomaterials especially fullerene which is reviewed [9].

Also, the influence of nanoscale materials on the pulmonary system was reported at a molecular level [10]. Furthermore, in vitro as well as in vivo tests of genotoxicity were determined for fullerene [11]. The reason why researchers are reporting against nanomaterials is coming from the fact that nanoscale particles are small as compared with cells and cellular organelles. With the activity of given nanoscale materials, it could penetrate then interact with the surroundings causing physical damage, could induce chemical interaction then a biological effect may exist and/or harmful inflammatory response. For example, oxidative stress caused by interacting nanoscale materials with lipids, carbohydrates, proteins and DNA causing possible damages. More precisely, the lipid peroxidation is considered as the most dangerous effects which could alter the properties of cell membrane as stated earlier [12-15]. It is also stated that high concentrations of nanomaterials such as metal oxides reveal some toxicity when used in quite high concentrations [16-18].

As an example of the effect of nanoscale materials on biological molecules, molecular modeling indicated that heme molecule is affected as a result of exposure to nanomaterials. The effect is varied from adsorbing state to complex one [19]. One of the leading techniques to investigate nanomaterials in different areas is molecular modeling. Such class of computational work is successfully providing physical, chemical and biological data about many systems and molecules in nanoscale [20-25]. The QSAR (Quantitative Structure Activity Relationships) approach is a computational tool that quantifies the relationship between a physicochemical property of a given structure and its biological activity [26]. It is basic concept is to calculate some molecular descriptors in terms mathematical equations which then elucidate directly and/or indirectly the biological activities of the studied molecules [27-28]. Recently, many researchers continue to calculate QSAR descriptors to assess the biological activity of many systems and molecules [29-33]. Based on the mentioned considerations molecular modeling is conducted to investigate the

possibility of interacting heme molecule and O_2, CO_2, CO, MgO, CoO, NiO, CuO and ZnO as examples for common and non-common species. A model molecule of heme molecule (H) interacting with each of the chosen molecules using PM6 quantum mechanical calculation is proposed as both adsorb and complex states.

2. MATERIALS AND METHODS

All calculations were conducted at semiemprical quantum mechanical calculations at PM6 level [34] via SCIGRESS 3.0. Software that is implemented at Spectroscopy Department, Physics Division, National Research Centre, NRC [35]. Model molecules of pristine heme molecule (H) and heme interacted with many common and non-common species via both adsorption and complex formation are built up. The interaction between the heme molecule and the added structure is always carried out through the Fe atom of heme. The selected entities are O_2, CO_2 and CO as common species and MgO, CoO, NiO, CuO and ZnO as non-familiar ones. The considered valence here is the divalent form of all the interested molecules. Then, they are geometrically optimized at PM6 level. Physical parameters such as charge (C), total dipole moment (TDM) and HOMO/LUMO band gap energy (ΔE) are considered. Finally, QSAR descriptors such as Final heat of formation (FF), Ionization potential (IP), Log P, Molar refractivity (MR), Surface area (A) and Volume (V) are also calculated at the same level.

3. RESULTS

3.1. Building Model Molecules.

The built heme molecule (H) depends on our previous work in [19]. **Figure 1** presents the heme structure as well as its suggested interactions with several species as adsorbing and complex states. Heme molecule is composed of porphyrin that is a ring-like organic structure and has a central Fe atom. This atom represents the active site of heme where it can attach to either oxygen or carbon dioxide gases in a reverse physical manner in order to satisfy its transportation function. **Figures (b-p)** show the interaction of heme and O_2, CO_2, CO, MgO, CoO, NiO, CuO and ZnO through its Fe active site, respectively.

3.2. Geometry Optimization.

The geometry of all the proposed structures is optimized at PM6 theoretical level. **Table 1** demonstrates some of the calculated physical parameters such as charge (C), total dipole moment (TDM) and band gap energy (ΔE).

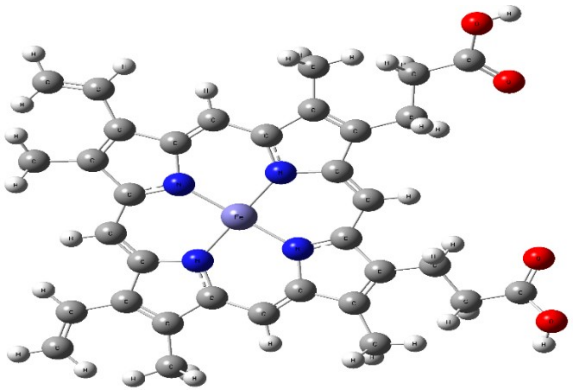

(a) H

Adsorb State (A)

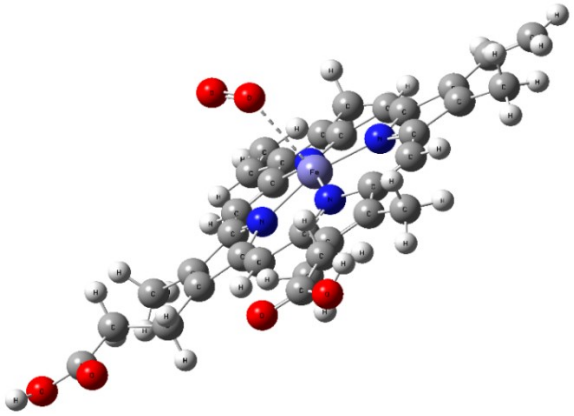

(b) H …..O_2 (A)

Complex State (C)

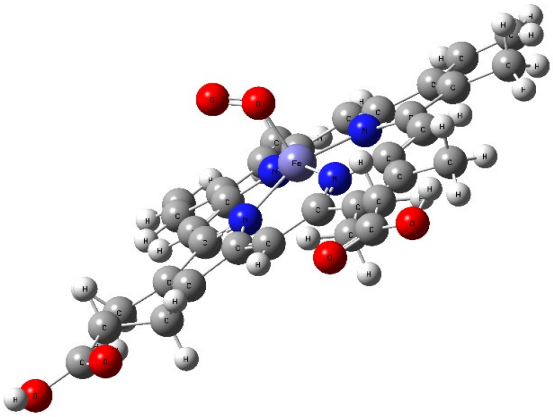

(c) H ----O_2 (C)

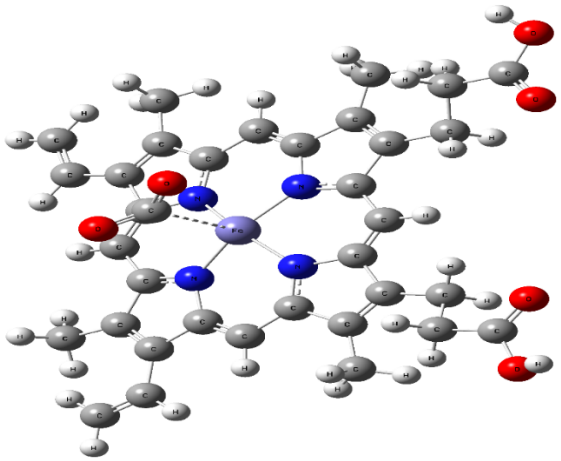

(d) H …….CO_2 (A)

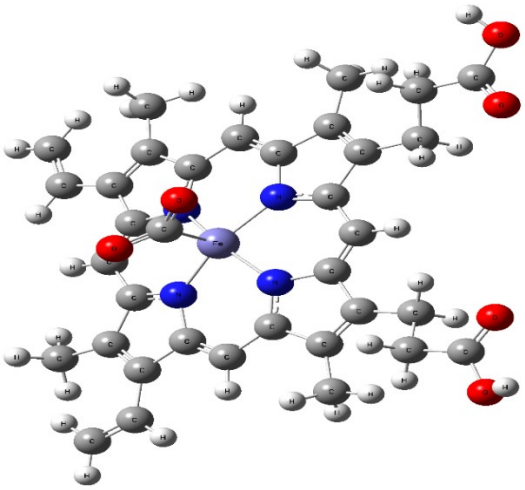

(e) H ----CO_2 (C)

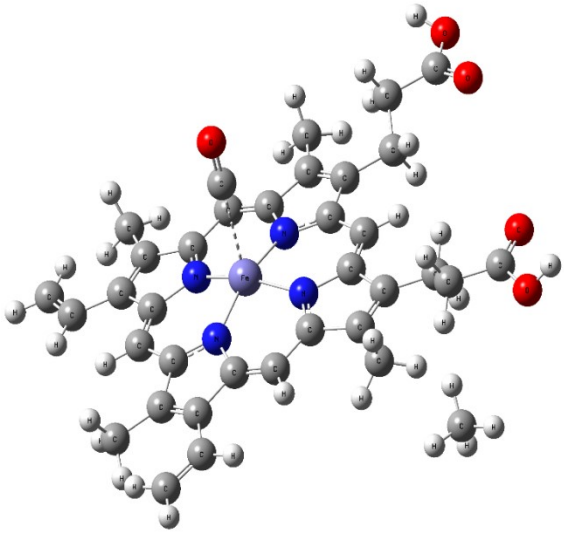

(f) H …….CO (A)

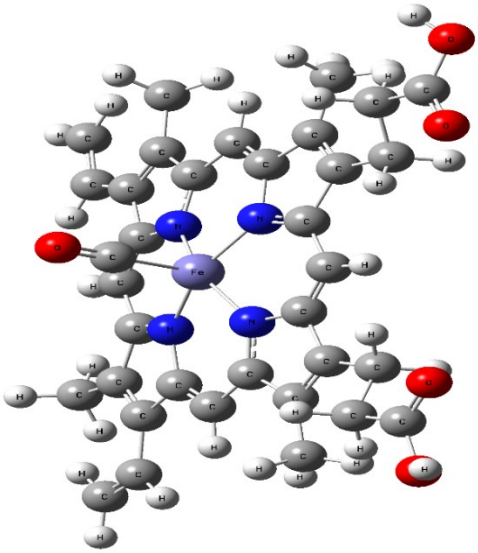

(g) H ----CO (C)

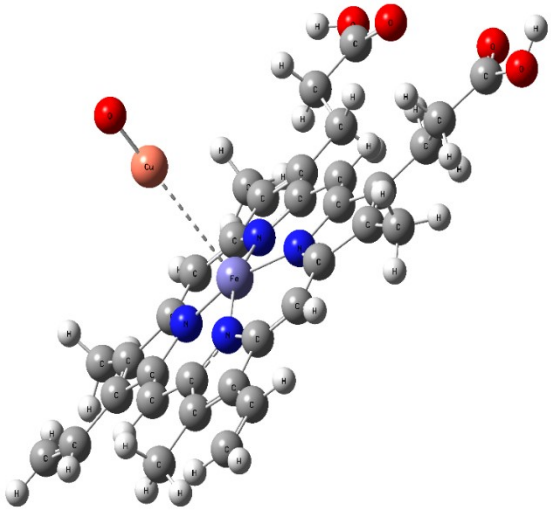

(h) H …….CuO (A)

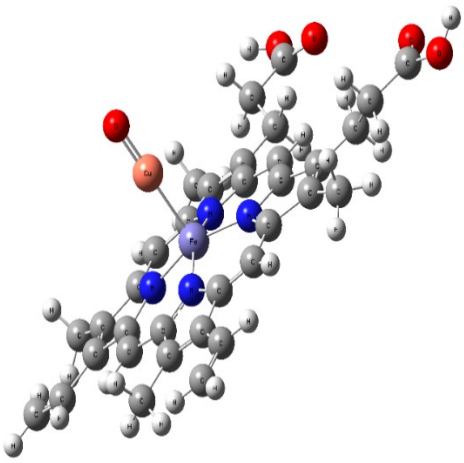

(i) H ----CuO (C)

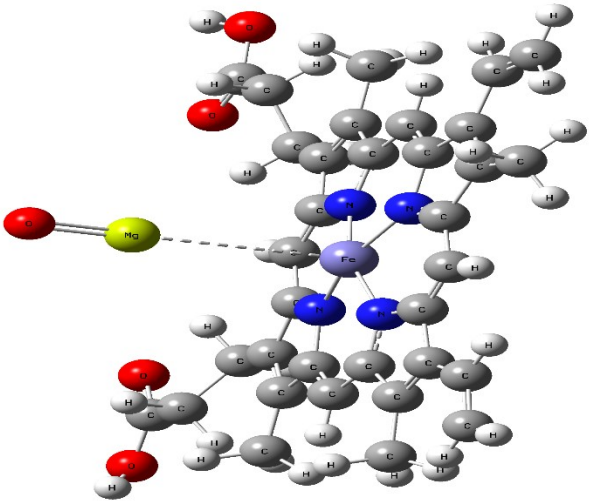

(j) H …….MgO (A)

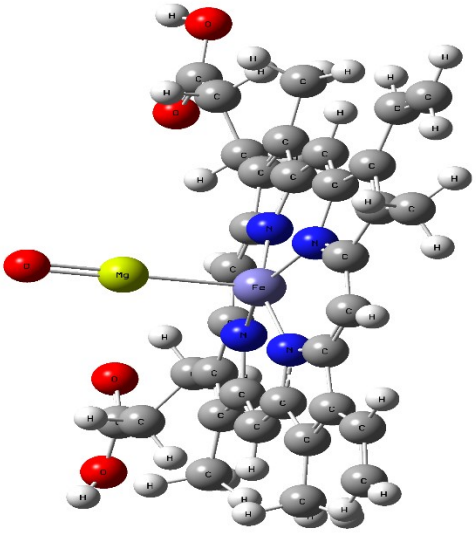

(k) H ----MgO (C)

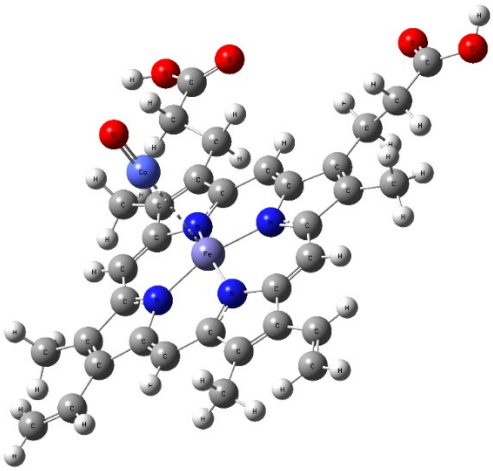

(l) H …….CoO (A)

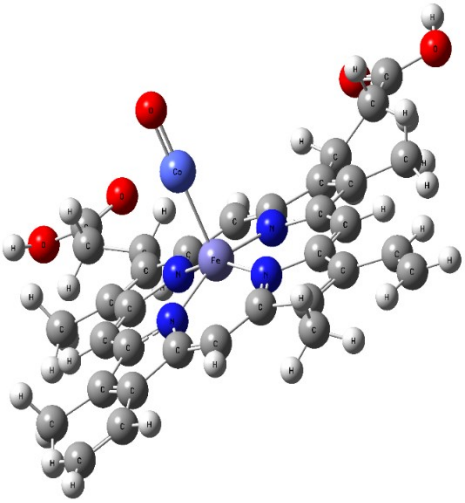

(m) H ----CoO (C)

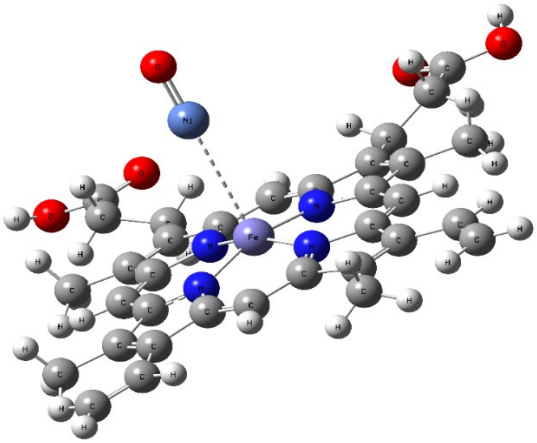

(m) H ……NiO (A)

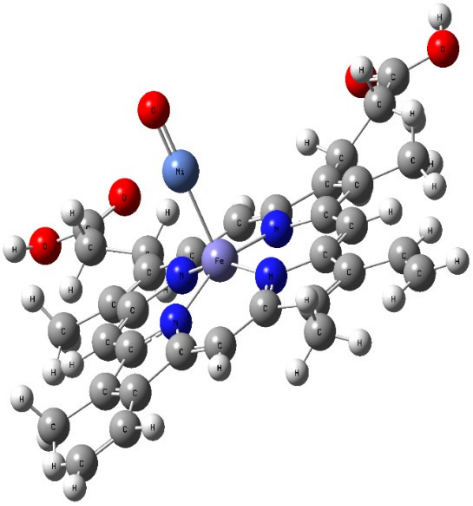

(n) H ----NiO (C)

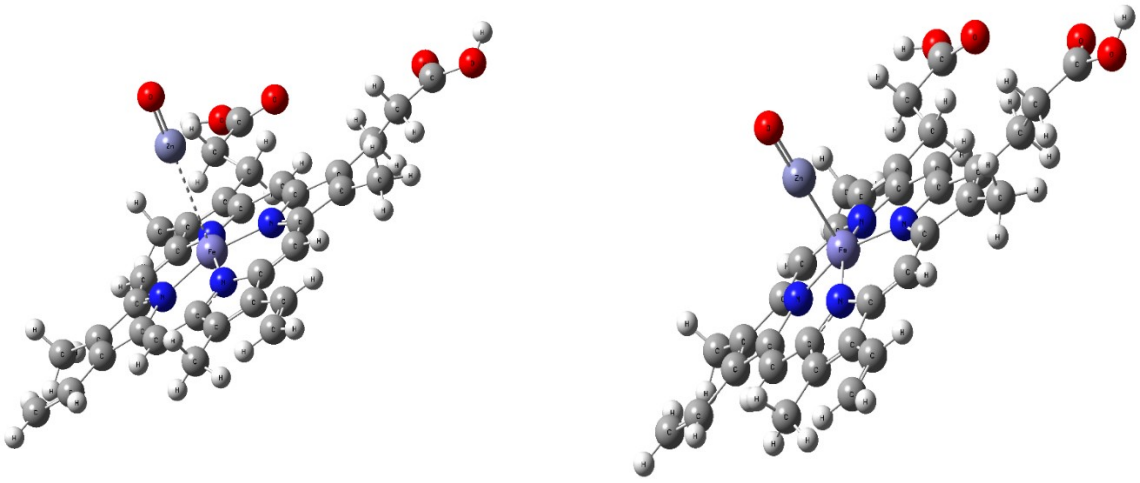

(o) H ……. ZnO (A) (p) H ----ZnO (C)

Figure 1. PM6 optimized (a) heme molecule (H), and its interaction with O_2, CO_2, CO, MgO, CoO, NiO, CuO and ZnO as adsorb state (A) on the left hand side and complex state (C) on the right hand side.

Table 1. PM6 calculated charge (C) as au, total dipole moment (TDM) as Debye and band gap energy (ΔE) as eV for heme molecule and its interaction structures with O_2, CO_2, CO, MgO, CoO, NiO, CuO and ZnO as adsorb and complex states.

Structure	C (au)	TDM (Debye)	ΔE (eV)
H	0	6.704	6.156
Interaction as adsorption			
H-O_2	0	6.099	6.414
H-CO_2	0	7.558	7.256
H-CO	2	5.483	4.686
H-MgO	0	7.195	6.545
H-CoO	0	36.171	1.739
H-NiO	0	9.609	6.329
H-CuO	0	8.606	4.955
H-ZnO	0	7.896	6.519
Interaction as complex			
H-O_2	-1	2.697	6.414
H-CO_2	-1	5.346	7.256
H-CO	1	4.453	4.686
H-MgO	-1	1.766	6.545
H-CoO	-1	71.053	1.739
H-NiO	-1	7.847	6.329
H-CuO	-1	2.759	4.955
H-ZnO	-1	75.109	6.519

Since, the considered valence for all the chosen molecules is the divalent form, hence not all the built structures are electrically neutral and some own charge either positive or negative. All the added compounds in the adsorb state have no electric charge except for the heme linked to carbon monoxide (H…CO) which has two positive charges. In the same manner for those in the complex state have negative charge except that attached to carbon monoxide (H---CO) that has positive charge. The negative charge on each of them results from gaining an electron so that they can form a strong covalent bond with Fe atom of the heme structure. Both total dipole moment (TDM) and HOMO/LUMO band gap energy (Δ E) are good physical references for structure reactivity. The calculated TDM for heme is 6.7 Debye. Adsorbing both O_2 and CO on heme decreases the TDM of their structures relative to heme, however adsorbing CoO increases greatly the resultant TDM where it reaches 36.2 Debye indicating a very reactive structure that may disturb the transportation function of heme molecule as it would be concerned to interact with further chemical structures more than performing its function. Adsorbing other species increases the resultant TDM with respect to pristine heme that would also affect negatively the transportation function of heme.

Formation of complexes between heme and O_2, MgO and CuO lowers greatly the TDM of the products reflecting lowering their activity that may lead to blocking the active site of heme which is responsible for gases transfer processes. However, forming a complex with CoO and ZnO elevates the TDM incredibly to 71.1 and 75.1 Debye, respectively. The HOMO/LUMO band gap of heme structure is 6.2 eV that decreases when adsorbing or complexing with CO, CoO and CuO reflecting higher reactivity for these structures. This would elevates their electrical conductivity that is characterized by

having several charged species. Adsorbing or complexing heme with O_2 has no impact on the band gap energy of both structures which reflects the suitability of heme structure for transferring processes of O_2 gas through the body.

3.3. QSAR Descriptors.

Quantitative structure-activity relationship QSAR offered simple and quite accessible scheme for investigating activities of biological compounds. It continues to be a topic of research work whereas someone would like to judge the biological activity [36-38]. QSAR parameters are conducted for the proposed structures at PM6 level in both adsorb and complex states. **Table 2** lists the calculated QSAR descriptors such as final heat of formation (FF), ionization potential (IP), Log P, molar refractivity (MR), surface area (SA) and volume (V).

Table 2. PM6 calculated QSAR descriptors including final heat of formation (FF) as kcal/mol, ionization potential (IP) as eV, Log P, molar refractivity (MR), surface area (SA) as A^2 and volume (V) as A^3 for heme molecule and its interaction structures with O_2, CO_2, CO, MgO, CoO, NiO, CuO and ZnO as adsorb and complex states.

Structure	FF (kcal/mol)	IP (eV)	log P	MR	SA (A^2)	V (A^3)
H	-52.745	-7.452	9.091	158.932	535.55	512.29
Interaction as adsorption						
H-O_2	-10.171	-7.217	-1.221	161.618	558.13	532.6
H-CO_2	-139.748	-7.574	-1.150	165.117	565.27	541.1
H-CO	-126.106	-0.591	-0.869	160.175	544.87	538.74
H-MgO	-116.089	-6.895	-0.700	158.321	535.550	536.49
H-CoO	-7.684	-6.514	8.740	160.375	598.66	569.62
H-NiO	18.991	-7.014	-0.869	160.175	561.8	545.65
H-CuO	56.705	-5.570	-0.869	160.175	562.75	547.28
H-ZnO	-77.746	-7.913	-0.869	160.175	558.89	544.39
Interaction as complex						
H-O_2	-29.111	-0.512	-1.221	161.525	545.22	536.08
H-CO_2	-189.163	-0.482	-1.150	165.118	548.4	544.13
H-CO	52.362	-8.232	-0.869	163.674	543.9	528.21
H-MgO	-161.976	-0.742	-0.700	157.910	562.45	544.3
H-CoO	-124.657	-6.795	8.740	160.175	616.69	581.89
H-NiO	-38.839	-0.512	-0.869	160.175	561.6	549.49
H-CuO	-77.303	-0.482	-0.869	159.316	575.4	551.08
H-ZnO	-124.729	-8.232	-0.869	160.175	615.61	581.18

Concerning FF that is usually defined as the heat change following the formation of a certain substance from its components [39]. It is 52.7 kcal for heme molecule while it reaches its lowest value for CO_2 and CO in the adsorb state with values -139.7, -126.1 kcal, respectively. While it has positive values for both NiO and CuO in the adsorb state indicating that their binding to heme in the adsorb state requires high amount of energy. For the calculated complex states, FF has its highest value for also heme bonded to O_2 with 29.1 kcal and smallest values for heme liked to CO_2 and MgO. On contrary, FF of heme attached to CO has a positive value of 52.36 kcal. Ionization potential (IP) is one of the QSAR descriptors that refer to structure reactivity. It is known as the energy required for ionizing a chemical structure. The resultant IP of heme is -7.5 eV and adsorbing CO_2 and ZnO decreases it to its minimum values of -7.6 and -7.9 eV, respectively. IP increases slightly as a result of adsorbing O_2, while it reaches its lowest value for adsorbing CO. Forming a complex structure with O_2, CO_2, MgO and NiO results in structures of the highest IP values indicating that it is difficult to form a complex structure with them. On the other hand, forming complex structures with CO and ZnO has the lowest IPs indicating they can complex with heme and block its site inhibiting it from performing its transportation function. Log P is abbreviation for the logarithm of the partition coefficient that used as hydrophilicity indicator. It equals to the ratio of a substance dissolved in organic solvent to that dissolved in aqueous solvents, hence positive Log P values refer to hydrophobic structures and negative ones indicate hydrophilic compounds. However, heme molecule seems to be hydrophobic, based on its positive Log P value, its interaction with the interested entities either in the complex or the adsorbed state results in hydrophilic structures except for that bonded to CoO in both cases referring that it's binding to heme is not preferred in the aqueous media. Heme attached with both O_2 and CO_2 in either adsorb or complex states produces the most hydrophilic structures among the calculated ones facilitating their attachment with heme in the biological aqueous environment. The interaction of heme with most of the other proposed compounds yields structures of nearly the same degree of hydrophilicity reflecting no preference for one of them to the others when binding to heme in the biological media. The calculated molar refractivity (MR) of heme equals 158.9 and its values when interacting with the chosen compounds in both adsorbed and complex states range from 157.9 for heme---MgO in a complex state to 165.1 for heme---CO_2 in both cases. Both of the calculated surface area and volume are among the geometrical QSAR parameters that are usually considered to assess the impact of bonding heme to the different species either in adsorb or complex states. The surface area and volume of heme molecule are calculated to be 535.6 A^2 and 512.3 A^3, respectively. The surface area of all the proposed structures either in adsorb or complex states is greater than that of heme except for MgO binding to heme through weak interaction that has nearly the same area. The calculated areas for the proposed structures can be categorized into three groups. Firstly, the surface area of some of them in the adsorbed state is higher than those in the complex form and it includes H-O_2, H-CO_2 and H-CO structures. Secondly,

a group includes structures whose areas in adsorb case is lower than in the complex and it involves H-MgO, H-CoO, H-CuO and ZnO compounds. Finally, H-NiO whose area does not affect by changing the connection type with heme. Regarding the variation in the volume, all the calculated volumes in the adsorbed state are lower than those in the complex one except for H-CO structure whose volume lower in the complex state.

The presented data empasizd that, molecular modeling show the ability to provide important physical, chemical and biological data for many systems and structures [40-45].

4. CONCLUSIONS

The present work studied the physical properties as well as the QSAR descriptors of heme molecule and heme interacted with familiar and non-familiar divalent structures using semiemprical quantum mechanical calculations at PM6 level. The interaction between the heme molecule and the added structure carried out through the Fe atom of heme as adsorb and complex states. Geometry optimization processes illustrate that adsorbing O_2 and CO on heme lowers their TDM helping heme in performing its transportation function and not interacting with other species. On the other hand, when CoO and ZnO interacting with heme the TDM of the resultant structures increase greatly reflecting high reactivity which may interact with other species more than performing its function. Therefore, interacting species other than O_2 may disturb the transportations function of heme structure. Electrical conductivity of heme increases at binding to CO, CoO and CuO that may affect negatively its performance, however interacting heme with O_2 have no impact on the band gap energy of both structures which reflects the suitability of heme structure for transferring processes of O_2 gas through the body. QSAR descriptors are investigated to study the molecules characteristics related to biological aspects. Results of IP regarding interaction of O_2 with heme ensure the TDM result that reflects lowering its activity. IP of H-CO adsorbed is the lowest indicating high reactivity while those of H-O_2, H-CO_2, H-MgO and H-NiO in the complex form are the highest values indicating that it is difficult to form a complex structure with them. Interacting heme with the proposed molecules converts it from hydrophobic into hydrophilic structure. Heme attached to both O_2 and CO_2 produces the most hydrophilic structures making them more preferred for heme in the biological aqueous environment. Furthermore, interaction of heme with other proposed compounds yields structures of the same degree of hydrophilicity reflecting no preference for one of them to the others when binding to heme in the biological media.

5. REFERENCES

1. Maruyama, S.; Miyauchi, Y.; Edamura, T.; lgarashi, Y.; Chiashi, S.; Murakami, Y. Synthesis of single-walled carbon nanotubes with narrow diameter-distribution from fullerene. *Chem Phys Lett* **2003**, *375*, 553-559, https://doi.org/10.1016/S0009-2614(03)00907-2.
2. Yu, M.F.; Lourie, O.; Dyer, M.J.; Moloni, K.; Kelly, T.F.; Ruoff, R.S. Strength and breaking mechanism of multiwalled carbon nanotubes under tensile load. *Science* **2000**, *287*, 637-640, https://doi.org/10.1126/science.287.5453.637.
3. Ferreira, F.V.; Mariano, M.; Lepesqueur, L.S.S.; Pinheiro, I.F.; Santos, L.G.; Burga-Sánchez, J.; Souza, D.H.S.; Koga-Ito, C.Y.; Teixeira-Neto, A.A.; Mei, L.H.I.; Gouveia, R.F.; Lona, L.M.F. Silver nanoparticles coated with dodecanethiol used as fillers in non-cytotoxic and antifungal PBAT surface based on nanocomposites. *Mater Sci Eng C* **2019**, *98*, 800-807, https://doi.org/10.1016/j.msec.2019.01.044.
4. Cobden, D.; Bockrath, M.; Chopra, N.; Zettle, A.; McEuen, P.; Rinzler, A.; Smalley, R. Spin Splitting and Even-Odd Effects in Carbon Nanotubes. *Phys Rev Lett* **1998**, *81*, 681-684, https://doi.org/10.1103/PhysRevLett.81.681.
5. Thiruvengadam, M.; Rajakumar, G.; Chung, Ill-Mi. Nanotechnology: current uses and future applications in the food industry. *3 Biotech* **2018**, *8*, 74, https://doi.org/10.1007/s13205-018-1104-7.
6. Lutolf, M.P.; Hubbell, J.A. Synthetic biomaterials as instructive extracellular microenvironments for morphogenesis in tissue engineering. *Nat Biotechnol* **2005**, *23*, 47–55, https://doi.org/10.1038/nbt1055.
7. Tekin, H.; Sanchez, J.G.; Landeros, C.; Dubbin, K.; Langer, R.; Khademhosseini, A. Controlling spatial organization of multiple cell types in defined 3D geometries. *Adv Mater Weinheim* **2012**, *24*, 5543–5547, https://doi.org/10.1002/adma.201201805.
8. Zorlutuna, P.; Annabi, N.; Camci-Unal, G.; Nikkhah, M.; Cha, J.M.; Nichol, J.W.; Manbachi, A.; Bae, H.; Chen, S.; Khademhosseini, A. Microfabricated biomaterials for engineering 3D tissues. *Adv Mater Weinheim* **2012**, *24*, 1782–1804, https://doi.org/10.1002/adma.201104631.
9. Kolosnjaj, J.; Szwarc, H.; Moussa, F. Bio-Applications of Nanoparticles. Springer, New York, **2007**, *620*, 168.
10. Fujita, K.; Morimoto, Y.; Ogam, A.; Myojyo, T.; Tanaka, I.; Shimada, M.; Wang, W.N.; Endoh, S.; Uchida, K.; Nakazato, T.; Yamamoto, K.; Fukui, H.; Horie, M.; Yoshida, Y.; Iwahashi, H.; Nakanishi, J. Gene expression profiles in rat lung after inhalation exposure to C60 fullerene particles. *Toxicology* **2009**, *258*, 47-55, https://doi.org/10.1016/j.tox.2009.01.005.
11. Shinohara, N.; Matsumoto, K.; Endoh, S.; Maru, J.; Nakanishi, J. In vitro and in vivo genotoxicity tests on fullerene C60 nanoparticles. *Toxicol Lett* **2009**, *191*, 289-296, https://doi.org/10.1016/j.toxlet.2009.09.012.
12. Donaldson, K.; Stone, V.; Seaton, A.; MacNee, W. Ambient particle inhalation and the cardiovascular system: Potential mechanisms. *Environ Health Perspect*. **2001**, *109*, 523–527, https://dx.doi.org/10.1289%2Fehp.01109s4523.
13. Dunford, R.; Salinaro, A.; Cai, L.Z.; Serpone, N.; Horikoshi, S.; Hidaka, H.; Knowland, J. Chemical oxidation and DNA damage catalysed by inorganic sunscreen ingredients. *FEBS Lett* **1997**, *418,* 87-90, https://doi.org/10.1016/S0014-5793(97)01356-2.
14. Fenech, M. The in vitro micronucleus technique. *Mutat Res Fund Mol Mech* **2000**, *455*, 81-95, https://doi.org/10.1016/S0027-5107(00)00065-8.
15. Xu, Z.; Wang, S.L.; Gao, H.W. Effects of nano-sized silicon dioxide on the structures and activities of three functional proteins. *J Hazard Mater* **2010**, *180*, 375-383, https://doi.org/10.1016/j.jhazmat.2010.04.042.
16. Yildirimer, L.; Thanh, N.T.; Loizidou, M.; Seifalian, A.M. Toxicology and clinical potential of nanoparticles. *Nano Today* **2011**, *6*, 585–607, https://doi.org/10.1016/j.nantod.2011.10.001.
17. Pan, Z.; Lee, W.; Slutsky, L.; Clark, R.A.F.; Pernodet, N.; Rafailovich, M.H. Adverse effects of titanium dioxide nanoparticles on human dermal fibroblasts and how

to protect cells. *Small* **2009**, *5*, 511–520, https://doi.org/10.1002/smll.200800798.
18. Liu, X.Q.; Tang, R.Z. Biological responses to nanomaterials: understanding nano-bio effects on cell behaviors. *J Drug Deliv* **2017,** *24,* 1-15, https://doi.org/10.1080/10717544.2017.1375577.
19. Elhaes, H.; Osman, O.; Ibrahim, M. Interaction of Nano Structure Material with Heme Molecule: Modelling Approach. *J Comput Theor Nanosci* **2012**, *9,* 901–905, http://dx.doi.org/10.1166/jctn.2012.2114.
20. Ibrahim, M.; Saleh, N.A.; Elshemey, W.M.; Elsayed, A.A. Hexapeptide Functionality of Cellulose as NS3 Protease Inhibitors. *Med Chem* **2012**, *8*, 826-830, https://doi.org/10.1166/jctn.2012.2114.
21. Youness, R.A.; Taha, M.A.; Elhaes, H.; Ibrahim, M. Molecular Modeling, FTIR Spectral Characterization and Mechanical Properties of Carbonated-Hydroxyapatite Prepared by Mechanochemical Synthesis. *Mater Chem Phys* **2017**, *190*, 209-218, https://doi.org/10.1016/j.matchemphys.2017.01.004.
22. Abdelsalam, H.; Teleb, N.H.; Yahia, I.S.; Zahran, H.Y.; Elhaes, H.; Ibrahim, M.A. First principles study of the adsorption of hydrated heavy metals on graphene quantum dots. *J Phys Chem Solids* **2019**, *130*, 32-40, https://doi.org/10.1016/j.jpcs.2019.02.014.
23. Abdelsalam, H.; Saroka, V.A.; Ali, M.; Teleb, N.H.; Elhaes, H.; Ibrahim, M.A. Stability and electronic properties of edge functionalized silicene quantum dots: A first principles study. *Physica E* **2019**, *108*, 339–346, https://doi.org/10.1016/j.physe.2018.07.022.
24. Abdelsalam, H.; Elhaes, H.; Ibrahim, M.A. First principles study of edge carboxylated graphene quantum dots. *Physica B* **2018**, *537*, 77-86, https://doi.org/10.1016/j.physb.2018.02.001.
25. Abdel-Gawad, F.K.; Osman, O.; Bassem, S.M.; Nassar, H.F.; Temraz, T.A.; Elhaes, H.; Ibrahim, M. Spectroscopic Analyses and Genotoxcity of Dioxins in the Aquatic Environment of Alexandria. *Mar Pollut Bull* **2018**, *127*, 618-625, https://doi.org/10.1016/j.marpolbul.2017.12.056.
26. Saleh, N.A.; Elhaes, H.; Ibrahim, M. Viral Proteases and Their Inhibitors, Chapter 2: Design and Development of Some Viral Protease Inhibitors by QSAR and Molecular Modeling Studies. *Elsevier* **2017**, 25-58. https://doi.org/10.1016/B978-0-12-809712-0.00002-2.
27. Welsh, W.J.; Tong, W.; Georgopoulos, P.G. *Computational Toxicology: Risk Assessment for Pharmaceutical and Environmental Chemicals*. Ekins, S., Ed.; John Wiley & Sons: Canada, **2007**, 153-175.
28. Garg, R.; Bhhatarai, B. QSAR and molecular modeling studies of HIV protease inhibitors. *Top Heterocycl Chem* **2006**, *3,* 181–271, https://doi.org/10.1007/7081_038.
29. Ponzoni, I.; Sebastián-Pérez, V.; Martínez, M.J.; Roca, C.; Pérez, C.C.; Cravero, F.; Vazquez, G.E.; Páez, J.A.; Díaz, M.F.; Campillo, N.E. QSAR Classification Models for Predicting the Activity of Inhibitors of Beta-Secretase (BACE1) Associated with Alzheimer's disease. *Sci Rep* **2019**, *9*, 9102, https://doi.org/10.1038/s41598-019-45522-3.
30. Alam, S.; Khan, F. 3D-QSAR, Docking, ADME/Tox studies on Flavone analogs reveal anticancer activity through Tankyrase inhibition. *Sci Rep* **2019**, *9*, https://doi.org/10.1038/s41598-019-41984-7.
31. Joseph, O.A.; Babatomiwa, K.; Niyi, A.; Olaposi, O.; Olumide, I. Molecular Docking and 3D Qsar Studies of C000000956 as a Potent Inhibitor of Bace-1. *Drug Res (Stuttg).* **2019**, *69*, 451-457, https://doi.org/10.1055/a-0849-9377.
32. Gul, A.; Akhter, Z.; Perveen, F.; Kalsoom, S.; Ansari, F.L.; Siddiq, M. Molecular Docking and Quantitative Structure Activity Relationship (QSAR) Studies of Some Newly Synthesized Poly (Azomethine) Esters. *Int J Pol Sci* **2019**, *2019*, https://doi.org/10.1155/2019/2103891.
33. Nóbrega, F.R.; Silva, L.V.; Filho, C.S.M.B.; Lima, T.C.; Castillo, Y.P.; Bezerra, D.P.; Lima, T.K.S.; Sousa, D.P. Design, Antileishmanial Activity, and QSAR Studies of a Series of Piplartine Analogues. *J Chem* **2019**, *2019,* https://doi.org/10.1155/2019/4785756.
34. Stewart, J.J.P. Optimization of parameters for semiempirical methods V: Modification of NDDO approximations and application to 70 elements. *J Mol Mod* **2007**, *13*, 1173-1213, https://doi.org/10.1007/s00894-007-0233-4.
35. Stewart J.J.P. SCIGRESS, Version 2.9.0, Fujitsu Limited, Sunnyvale, Calif, USA **2009**.
36. Ma, W.; Wang, Y.; Chu, D.; Yan, H. 4D-QSAR and MIA-QSAR study on the Bruton's tyrosine kinase (Btk) inhibitors. *J Mol Graph Model* **2019**, *92*, 357-362, https://doi.org/10.1016/j.jmgm.2019.08.009.
37. Elrhayam, Y.; Elharfi, A. 3D-QSAR studies of the chemical modification of hydroxyl groups of biomass (cellulose, hemicelluloses and lignin) using quantum chemical descriptors. *Heliyon* **2019**, *5*, e02173, https://doi.org/10.1016/j.heliyon.2019.e02173.
38. Muthukumaran, P.; Rajiniraja, M. Aug-MIA-QSAR based strategy in bioactivity prediction of a series of flavonoid derivatives as HIV-1 inhibitors. *J Theor Biol* **2019**, *469*, 18-24, https://doi.org/10.1016/j.jtbi.2019.02.019.
39. El-Haes, H.; Saleh, N.A.; Omar, A.; Ibrahim, M. Molecular spectroscopic study of fulleropyrrolidine carbodithioic acid. J. Comput. Theor. Nanosci. **2014**, *11*, 2136-2140. https://doi.org/10.1166/jctn.2014.3618.
40. Badry, R.; El-Khodary, S.; Elhaes, H.; Nada, N.; Ibrahim, M. The Influence of Moisture on the Electronic Properties of Monomer, Dimer, Trimer and Emeraldine Base Sodium Carboxymethyl Cellulose. *Egyptian Journal of Chemistry* **2019**, *62*, 39-56, https://doi.org/10.33263/LIANBS82.553557.
41. Grenni, P.; Caracciolo, A.B.; Mariani, L.; Cardoni, M.; Riccucci, C.; Elhaes, H.; Ibrahim, M.A. Effectiveness of a new green technology for metal removal from contaminated water. *Microchemical Journal* **2019**, *147*, 1010-1020, https://doi.org/10.1016/j.microc.2019.04.026.
42. Afzal, M.A.F.; Hachmann, J. Benchmarking DFT approaches for the calculation of polarizability inputs for refractive index predictions in organic polymers. *Phys. Chem. Chem. Phys.* **2019**, *21*, 4452-4460, https://doi.org/10.1039/C8CP05492D.
43. Fahim, A.M.; Shalaby M.A.; Ibrahim, M. Microwave-assisted synthesis of novel 5-aminouracil-based compound with DFT calculations. *J. Mol. Struct*. **2019**, *1194*, 211-226, https://doi.org/10.1016/j.molstruc.2019.04.078.
44. Arı, H.; Büyükmumcu, Z. Comparison of DFT functionals for prediction of band gap of conjugated polymers and effect of HF exchange term percentage and basis set on the performance. *Computational Materials Science* **2017**, *138,* 70-76, https://doi.org/10.1016/j.commatsci.2017.06.012.
45. Youness, RA.; Taha, MA.; Ibrahim, M. In vitro bioactivity, molecular structure and mechanical properties of zirconia-carbonated hydroxyapatite nanobiocomposites sintered at different temperatures, Materials Chemistry and Physics, 2020, 239,122011. https://doi.org/10.1016/j.matchemphys.2019.122011.

6. ACKNOWLEDGEMENTS

This work is carried out in the frame of the ASRT-JINR bilateral project “Molecular Modeling Analyses of the Effect of Nano Metal Oxides on Biological Molecules”.